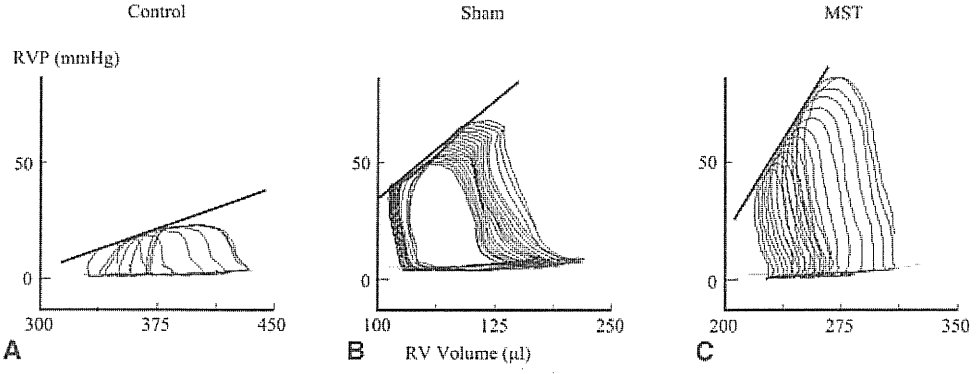

FIGURE 1. Representative pressure–volume loops of the control (A), sham (B), and myoblast sheet transplantation (*MST*; C) groups under different loading conditions. The slope of the end-systolic pressure–volume relationship is displayed as a *black straight line*. The correlation of the end-diastolic pressure–volume relationship is displayed as a *green monoexponential curve*. *RVP*, Right ventricular pressure; *RV*, right ventricle.

blood vessels. The right ventricle was carefully separated from the left ventricle and intraventricular septum (IVS). The fresh ventricular tissues were immediately blotted dry and weighted separately to determine the degree of RV hypertrophy based on 2 parameters: RV wall weight/body weight (RV/BW) and RV wall weight/LV and IVS wall weight (RV/LV+IVS).

Tissue specimens were obtained from the endocardium, the midwall, and the epicardium of the RV anterior wall in cross-sections, cut into 5-μm-thick sections, and stained with hematoxylin and eosin for morphologic analysis, including measurement of RV wall thickness, periodic acid–Schiff staining to measure the short-axis length of the RV myocardial cell, Factor VIII–related antigen staining (Dako EPOS anti-human Von Willebrand factor/HRP; Dako Cytomation, Glostrup, Denmark) to quantify capillary vascular density, and Masson trichrome staining for determination of the amount of interstitial and myocardial fibrosis. The percentage of interstitial and myocardial fibrosis were assessed by a computer-based method[23,24] with the use of a software filter (Mac Scope Software; MITANI Corp, Tokyo, Japan), which can recognize the distinct color shades. The number of pixels of the blue-stained collagen area was calculated, then divided by the total number of pixels in a field. Each 3 fields of the endocardial, epicardial, and mid layers of the RV wall per slide were analyzed and then averaged.

RT-PCR

Total RNA was isolated from the stored specimens by using the RNeasy Mini Kit (Qiagen, Hilden, Germany) and reverse transcribed with Omniscript Reverse Transcriptase (Qiagen). RT-PCR was performed with the ABI PRISM 7700 (Applied Biosystems, Foster City, Calif). Measurement of the mRNA expression of hepatocyte growth factor (HGF) and vascular endothelial growth factor (VEGF) was performed in triplicate. The results are expressed after normalization for glyceraldehyde-3-phosphate dehydrogenase (GAPDH).

Statistical Analysis

All data were expressed as the mean ± SEM and range. Student's unpaired *t* test or analysis of variance for parametric values was used to compare group means.

RESULTS

Pressure Overload and Hypertrophy of the Right Ventricle After PAB

After PAB, a weight analysis showed the heart weight/BW, RV/BW, and RV/(LV+IVS) weight ratios in the sham and MST groups to be similar and significantly higher than in the control group (Table 1). Both the sham and MST groups showed a significantly increased end-systolic pressure and dP/dtmax than seen in the control group (Table 2).

Hemodynamic Effects of MST

The baseline indices revealed that end-diastolic pressure and τ values were significantly increased only in the sham group in comparison with those in the control group but not in the MST group (Table 2). Typical examples of the pressure–volume loop in each group are presented in Figure 1. The pressure–volume loop analysis revealed that the ESPVR and PRSW values significantly increased both in the sham and MST groups. However, the EDPVR value significantly increased only in the sham group (control vs sham vs MST groups: 8.6 ± 2.9 vs 16.1 ± 4.5 vs 7.6 ± 2.4/mL; $P < .05$ in the control and MST groups vs the sham group; Table 2).

Histologic Effects of MST

Whole heart findings showed the RV wall thickened, the cavity enlarged, and the IVS shifted toward the left side in the sham and MST groups (Figure 2, *A*). In the MST group transplanted MSs were observed as an elastic thin layer on the epicardium (Figure 2, *B*). The RV wall thickness and myocardial cell size in the sham and MST groups were similar and significantly higher than in the control group (Figure 2, *C–E*).

TABLE 1. Weight analysis at the fourth week after the operation

Group	Control	Sham	MST
HW/BW (mg/g)	2.62 ± 0.09	3.53 ± 0.50*	4.03 ± 0.59*
RV/BW (mg/g)	0.54 ± 0.15	1.62 ± 0.42*	1.65 ± 0.32*
RV/(IVS+LV)	0.27 ± 0.08	0.69 ± 0.11*	0.69 ± 0.09*

MST, Myoblast sheet transplantation; *HW*, heart weight; *BW*, body weight; *RV*, right ventricle; *IVS*, interventricular septum; *LV*, left ventricle. *$P < .05$ versus the control group.

TABLE 2. Hemodynamic indices at the fourth week after the operation

Group	Control	Sham	MST
Basic hemodynamic indices			
HR (beats/min)	280 ± 72	233 ± 34	249 ± 65
ESP (mm Hg)	22.8 ± 2.9	82.3 ± 11.8*	78.7 ± 13.2*
EDP (mm Hg)	2.4 ± 1.4	10.3 ± 3.1*†	5.0 ± 3.7
dP/dtmax (mm Hg/s)	1301 ± 206	3197 ± 597*	3352 ± 1332*
dP/dtmin (mm Hg/s)	−997 ± 210	−2466 ± 582*	−2682 ± 828*
τ (ms)	7.9 ± 2.7	11.1 ± 2.5*†	7.6 ± 1.2
Load-independent parameters analyzed by PV loop			
ESPVR (mm Hg/mL)	538 ± 196	857 ± 305*	967 ± 201*
EDPVR (/mL)	8.6 ± 2.9	16.1 ± 4.5*†	7.6 ± 2.4
PRSW (mm Hg)	17.0 ± 4.1	40.2 ± 19.6*	40.8 ± 13.6*
PRSW/RV (mm Hg/kg)	88.3 ± 23.9	71.5 ± 31.3	73.6 ± 28.8

MST, Myoblast sheet transplantation; *HR*, heart rate; *ESP*, end-systolic pressure; *EDP*, end-diastolic pressure; *PV*, pressure–volume; *ESPVR*, end-systolic pressure–volume relationship; *EDPVR*, end-diastolic pressure–volume relationship; *PRSW*, preload-recruitable stroke work; *RV*, right ventricular weight. *P < .05 versus the control group. †P < .05 versus the MST group.

Factor VIII stain showed that myocardial capillary vascular density showed no significant difference at the mid layer and endocardial layer (Figure 3, *B* and *C*), but it was significantly higher in the MST group than in the other 2 groups at the epicardial layer (Figure 3, *A*). Hence, total capillary density in the MST group was significantly higher than in the other 2 groups (control vs sham vs MST groups: 262 ± 98 vs 271 ± 289 vs 823 ± 708; P <0.05 in the control and sham groups vs the MST group; Figure 3, *D*).

Periodic acid–Schiff staining demonstrated significant interstitial fibrosis of the right ventricle in both the sham and MST groups, but the percentage of fibrosis in the

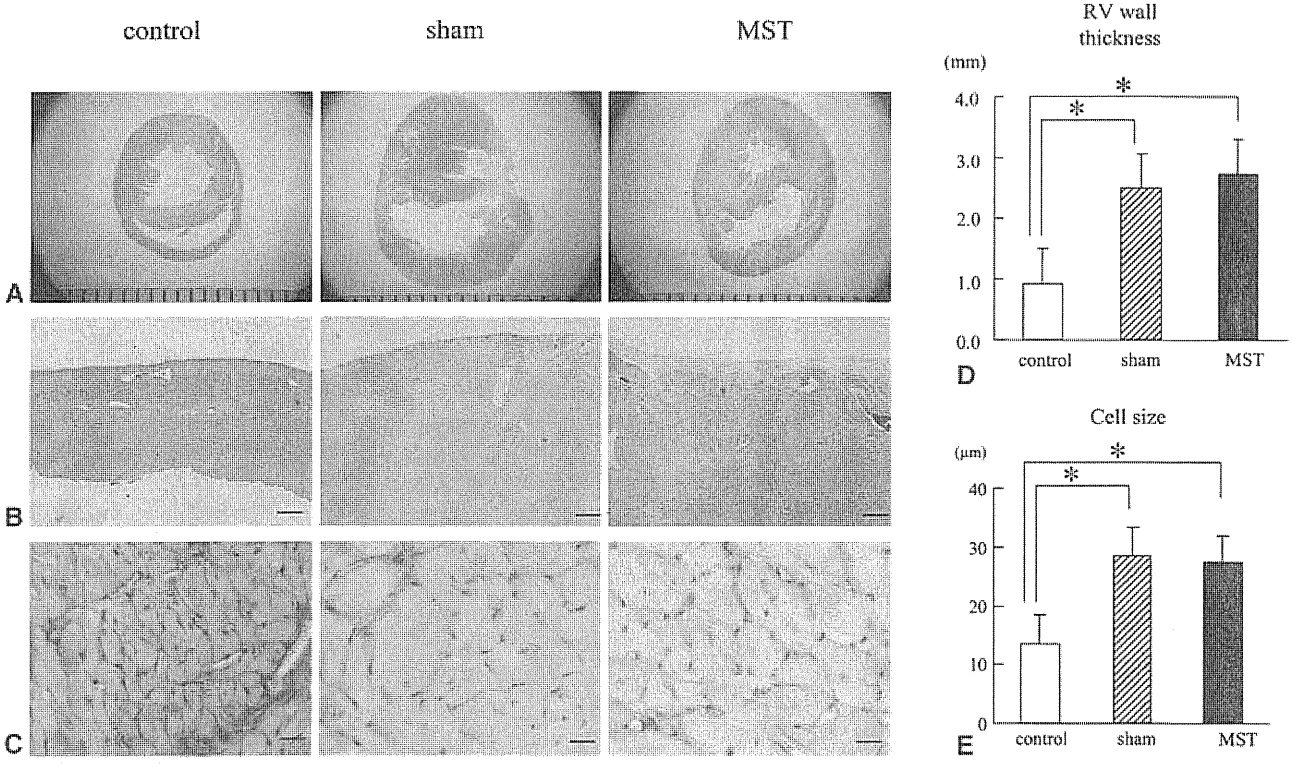

FIGURE 2. Macroscopic photographs of hematoxylin and eosin–stained sections showing right ventricular *(RV)* wall thickening, cavity enlarging, and the intraventricular septum shifting towered the left side in the sham and myoblast sheet transplantation *(MST)* groups (A and D). Photomicrographs (40×, scale bar = 200 μm) of hematoxylin and eosin–stained sections showed a fibrous organized thin layer on the epicardium in the myoblast sheet transplantation group (B). Photomicrographs (400×, scale bar = 20 μm) of periodic acid–Schiff–stained sections showed significantly hypertrophied ventricular myocytes in the sham and myoblast sheet transplantation groups (C and E). *P < .05 (n = 10).

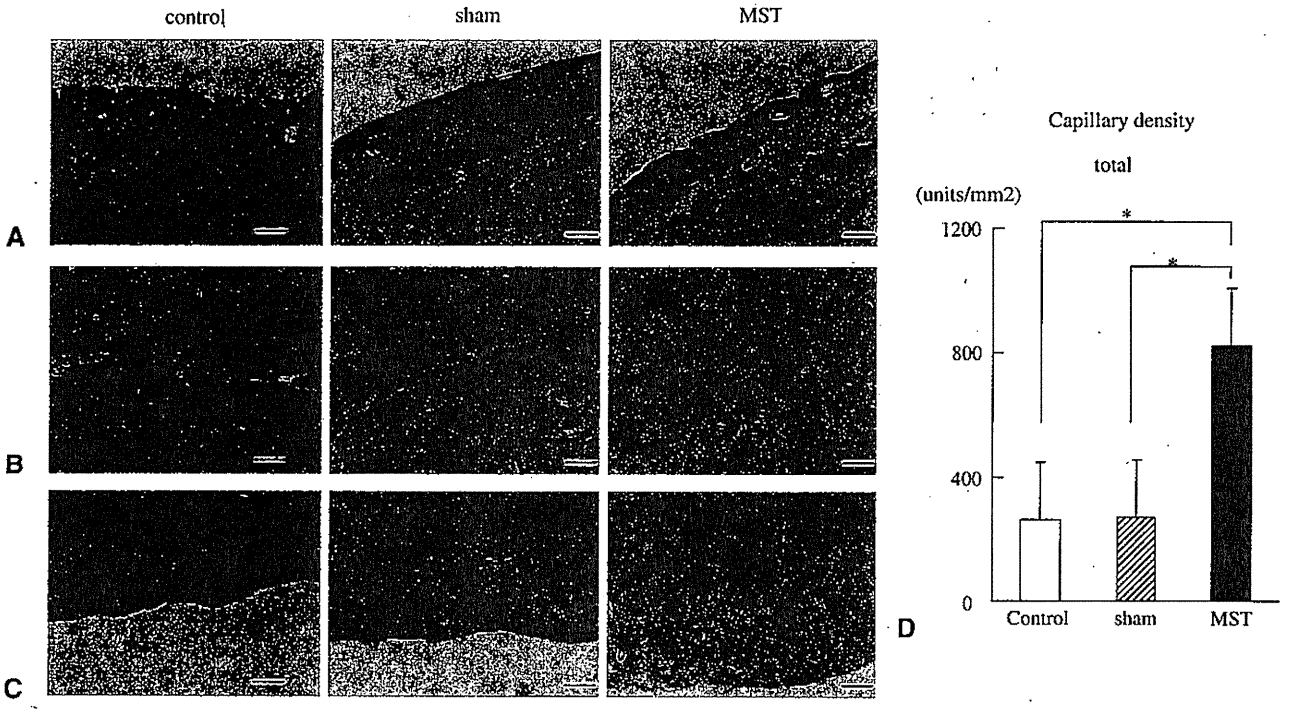

FIGURE 3. Representative photomicrographs (100×, scale bar = 100 μm) of Factor VIII–stained epicardial layer (A), mid layer (B), and endocardial layer (C). Neovascularization occurred at the epicardial layer in the myoblast sheet transplantation *(MST)* group (D). *$P < .05$ (n = 10).

MST group was significantly less than that in the sham group (control vs sham vs MST groups: 4.8% ± 1.1% vs 24.5% ± 10.0% vs 19.0% ± 5.1%; $P < .05$ between each 2 groups; Figure 4, *A* and *E*). Aggregated endomyocardial fibrosis was detected only in the sham group (endomyocardial percentage of fibrosis, control vs sham vs MST groups: 5.7% ± 0.1% vs 31.5% ± 8.4% vs 18.6% ± 5.9%; $P < .01$ in the control and MST groups vs the sham group; Figure 4, *B–D* and *F*).

RT-PCR

The expression of HGF and VEGF mRNA in the MST group was significantly higher than in the sham group (control vs sham vs MST groups: HGF, 0.00009 ± 0.00008 vs 0.00041 ± 0.00030 vs 0.00073 ± 0.00031/GAPDH [$P < .05$ in each group]; *VEGF*, 0.00242 ± 0.00164 vs 0.00329 ± 0.00181 vs 0.00512 ± 0.00113/GAPDH [$P < .05$ in the control and sham group vs the MST group]; Figure 5).

DISCUSSION

This study demonstrated that skeletal MST improved diastolic function in a pressure-overloaded right heart model in rats by means of PAB. This conclusion is supported by the following evidence: (1) the diastolic function was significantly improved based on hemodynamic assessment and pressure–volume loop analysis; (2) interstitial and endocardial fibrosis was ameliorated, and capillary vascular density of the epicardial layer was increased; and (3) myocardial gene expression of HGF and VEGF was significantly increased. MST has been shown to have therapeutic effects in several models of LV failure.[14-16] However, the present results are the first to show evidence that MST is effective for the treatment of RV dysfunction resulting from chronic pressure overload.

Prolonged RV pressure overload promotes unique morphologic, histologic, and functional changes. The mechanical stimulation of pressure overload extends the myocardium, which leads to diastolic dysfunction.[21] Simultaneously, hypertrophied myocardium upregulates the release of various chemical mediators,[17] which induce further myocardial expansion, apoptosis, necrosis, and fibrosis, finally resulting in RV decompensation. Otherwise, ventricular hypertrophy itself reduces the coronary flow reserve (CFR) and leads to coronary microcirculatory dysfunction.[25] As studies on the left ventricle show, this phenomenon is detected particularly in the subendocardium.[26] The shortage of CFR induces myocardial cellar mortality and endocardial fibrosis, which accelerates ventricular dysfunction. The present and previous data indicate that transplanted elastic cells initially improved ventricular stiffness[14] and preserved CFR in the hypertrophied myocardium, both of which generate a synergistic effect of the suppression of myocardial cell death and fibrosis, especially at the endocardial layer. Although an angiogenetic effect was observed with the increased myocardial gene expression of HGF and VEGF, we speculate this does not increase endocardial coronary flow directly because increased

ETBS

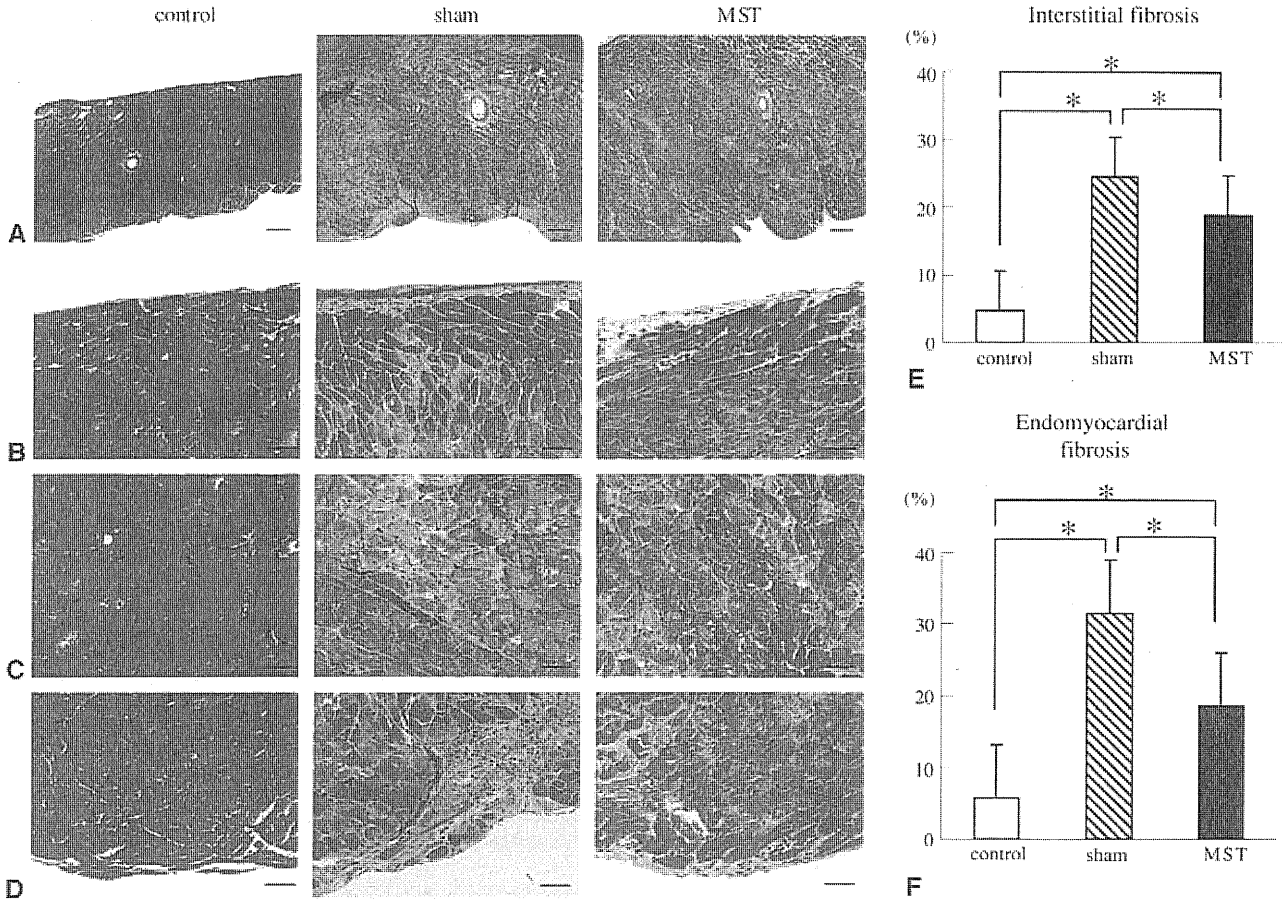

FIGURE 4. Representative photomicrographs of Masson's trichrome–stained transmural layer (A; 40×, scale bar = 200 μm), epicardial layer (B), mid layer (C), and endocardial layer (D; 200×, scale bar = 50 μm) for evaluation of interstitial (E) and endomyocardial (F) fibrosis. *$P < .05$ (n = 10).

capillary density was only seen at epicardial layer. These new capillaries might increase the blood supply to the transplanted myoblasts and prolong their survival.[13]

As several LV studies have previously shown, Lamberts and colleagues[27] revealed the strict relationship between RV chamber stiffness and the degree of myocardial fibrosis. In their report they also described that prevention or reduction of RV fibrosis improved RV diastolic dysfunction. Although we could not show any individual correlation between collagen contents and hemodynamic parameters in regard to diastolic function, these findings strongly support our results. Therefore we would like to emphasize that the suppression of fibrosis improved the RV diastolic function.

The hemodynamic assessment of cardiac performance of a hypertrophied right ventricle has not been established. Various attempts have been made; however, it is still necessary to perform cardiac catheterization to evaluate hemodynamics, especially regarding diastolic function.[28,29] Leeuwenburgh and associates[4] showed that RV compliance deteriorated in a lamb model and described τ and EDPVR values to be useful indicators for diastolic function. Gaynor

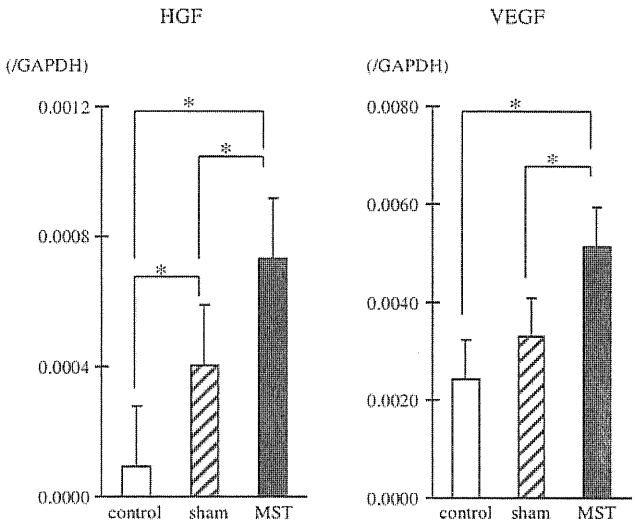

FIGURE 5. RT-PCR for evaluation of neurohormonal factor gene expression. The results are expressed after normalization for GAPDH. *HGF*, Hepatocyte growth factor; *VEGF*, vascular endothelial growth factor. *$P < .05$ (n = 10).

ET/BS

and coworkers[5] also showed an increase of EDPVR in a dog model of PAB. The current results are consistent with these reports. Therefore these data appear to be reliable.

On the other hand, the assessment of systolic function still remains controversial. In this study we showed that ESPVR (Ees) and PRSW were significantly increased in sham groups, as previously reported.[30] However, Dell'Italia and Walsh[31] pointed out that in the assessment of RV contractility, the slope of ESPVR (Ees) was different from the slope of the maximum time-varying elastance, which better reflected the RV contractility than Ees. In addition to Ees, PRSW is thought to be an optimal parameter of ventricular contractility. However, we might have to consider the discrepancy of the cardiac mass between normal and hypertrophied hearts because ventricular SW should be assessed as a per-unit cardiac mass. We tried to calculate the PRSW divided for each animal's RV weight, which revealed there was no statistical significance among the 3 groups (control vs sham vs MST groups: 88.3 ± 23.9 vs 71.5 ± 31.3 vs 73.6 ± 28.8 mm Hg/kg; Table 2). Hence it is hard to say that the RV pressure load induced a further improvement in RV contractility.

We need further investigation to apply this method to clinical RV failure because we did not ascertain the effect of MST on RV systolic function. Nevertheless, enormous fibrosis was seen in the sham group, and systolic function was still compensated until the timing of hemodynamic evaluation. However, previous reports showed that MST had an excellent effect on LV contractility.[14-16] Therefore we expect that this method might become a novel and potentially effective treatment strategy for patients with RV failure.

In conclusion, chronic pressure overload to the right ventricle caused hypertrophy and impaired diastolic function in rats. Skeletal MST attenuated diastolic dysfunction, which was mainly caused by suppressed interstitial and endocardial fibrosis. This method might become a novel strategy for the myocardial regeneration of RV failure in patients with CHD in the future.

We thank Mrs Masako Yokoyama for her expert assistance with RT-PCR and Kazuhiro Takekita and Takeshi Miki for technical support in creating the tissue-engineered skeletal MSs.

ETBS

References

1. Bolger AP, Coats AJ, Gatzoulis MA. Congenital heart disease: the original heart failure syndrome. *Eur Heart J*. 2003;24:970-6.
2. Murphy JG, Gersh BJ, Mair DD, Fuster V, McGoon MD, Ilstrup DM, et al. Long-term outcome in patients undergoing surgical repair of tetralogy of Fallot. *N Engl J Med*. 1993;329:593-9.
3. Gatzoulis MA, Balaji S, Webber SA, Siu SC, Hokanson JS, Poile C, et al. Risk factors for arrhythmia and sudden cardiac death late after repair of tetralogy of Fallot: a multicentre study. *Lancet*. 2000;356:975-81.
4. Leeuwenburgh BP, Steendijk P, Helbing WA, Baan J. Indexes of diastolic RV function: load dependence and changes after chronic RV pressure overload in lambs. *Am J Physiol Heart Circ Physiol*. 2002;282:1350-8.
5. Gaynor SL, Maniar HS, Bloch JB, Steendijk P, Moon MR. Right atrial and ventricular adaptation to chronic right ventricular pressure overload. *Circulation*. 2005;112:212-8.
6. Deanfield JE, Ho SY, Anderson RH, McKenna WJ, Allwork SP, Hallidie-Smith KA. Late sudden death after repair of tetralogy of Fallot: a clinicopathologic study. *Circulation*. 1983;67:626-31.
7. Babu-Narayan SV, Kilner PJ, Li W, Moon JC, Goktekin O, Davlouros PA, et al. Ventricular fibrosis suggested by cardiovascular magnetic resonance in adults with repaired tetralogy of Fallot and its relationship to adverse markers of clinical outcome. *Circulation*. 2006;113:405-13.
8. Chowdhury UK, Sathia S, Ray R, Singh R, Pradeep KK, Venugopal P. Histopathology of the right ventricular outflow tract and its relationship to clinical outcomes and arrhythmias in patients with tetralogy of Fallot. *J Thorac Cardiovasc Surg*. 2006;132:270-7.
9. Taylor DA, Atkins BZ, Hungspreugs P, Jones TR, Reedy MC, Hutcheson KA, et al. Regenerating functional myocardium: improved performance after skeletal myoblast transplantation. *Nat Med*. 1998;4:929-33.
10. Menasche P, Hagege AA, Scorsin M, Pouzet B, Desnos M, Duboc D, et al. Myoblast transplantation for heart failure. *Lancet*. 2001;357:279-80.
11. Hagege AA, Marolleau JP, Vilquin JT, Alheritiere A, Peyrard S, Duboc D, et al. Skeletal myoblast transplantation in ischemic heart failure: long-term follow-up of the first phase I cohort of patients. *Circulation*. 2006;114:108-13.
12. Okano T, Yamada N, Sakai H, Sakurai Y. A novel recovery system for cultured cells using plasma-treated polystyrene dishes grafted with poly(N-isopropylacrylamide). *J Biomed Mater Res*. 1993;27:1243-51.
13. Miyagawa S, Sawa Y, Sakakida S, Taketani S, Kondoh H, Memon IA, et al. Tissue cardiomyoplasty using bioengineered contractile cardiomyocyte sheets to repair damaged myocardium: their integration with recipient myocardium. *Transplantation*. 2005;80:1586-95.
14. Memon IA, Sawa Y, Fukushima N, Matsumiya G, Miyagawa S, Taketani S, et al. Repair of impaired myocardium by means of implantation of engineered autologous myoblast sheets. *J Thorac Cardiovasc Surg*. 2005;130:1333-41.
15. Kondoh H, Sawa Y, Miyagawa S, Sakakida-Kitagawa S, Memon IA, Kawaguchi N, et al. Longer preservation of cardiac performance by sheet-shaped myoblast implantation in dilated cardiomyopathic hamsters. *Cardiovasc Res*. 2006;69:466-75.
16. Hata H, Matsumiya G, Miyagawa S, Kondoh H, Kawaguchi N, Matsuura N, et al. Grafted skeletal myoblast sheets attenuate myocardial remodeling in pacing-induced canine heart failure model. *J Thorac Cardiovasc Surg*. 2006;132:918-24.
17. Lekanne Deprez RH, van den Hoff MJ, de Boer PA, Ruijter PM, Maas AA, Chamuleau RA, et al. Changing patterns of gene expression in the pulmonary trunk-banded rat heart. *J Mol Cell Cardiol*. 1998;30:1877-88.
18. Sato T, Shishido T, Kawada T, Miyano H, Miyashita H, Inagaki M, et al. ESPVR of in situ rat left ventricle shows contractility-dependent curvilinearity. *Am J Physiol Heart Circ Physiol*. 1998;274:H1429-34.
19. Baan J, van der Velde ET, de Bruin HG, Smeenk GJ, Koops J, van Dijk AD, et al. Continuous measurement of left ventricular volume in animals and humans by conductance catheter. *Circulation*. 1984;70:812-23.
20. Suga H, Sagawa K. Instantaneous pressure-volume relationships and their ratio in the excised, supported canine left ventricle. *Circ Res*. 1974;35:117-26.
21. Gaasch WH, Cole JS, Quinones MA, Alexander JK. Dynamic determinants of left ventricular diastolic pressure-volume relations in man. *Circulation*. 1975;51:317-23.
22. Glower DD, Spratt JA, Snow ND, Kabas JS, Davis JW, Olsen CO, et al. Linearity of the Frank-Starling relationship in the intact heart: the concept of preload recruitable stroke work. *Circulation*. 1985;71:994-1009.
23. Hoyt RH, Collins SM, Skorton DJ, Ericksen EE, Conyers D. Assessment of fibrosis in infarcted human hearts by analysis of ultrasonic backscatter. *Circulation*. 1985;71:740-4.
24. Vasiljević JD, Popović ZB, Otasević P, Popović ZV, Vidaković R, Mirić M, et al. Myocardial fibrosis assessment by semiquantitative, point-counting and computer-based methods in patients with heart muscle disease: a comparative study. *Histopathology*. 2001;38:338-43.
25. Murray PA, Vatner SF. Reduction of maximal coronary vasodilator capacity in conscious dogs with severe right ventricular hypertrophy. *Circ Res*. 1981;48:25-33.
26. Rajappan K, Rimoldi OE, Dutka DP, Ariff B, Pennell DJ, Sheridan DJ, et al. Mechanisms of coronary microcirculatory dysfunction in patients with aortic stenosis and angiographically normal coronary arteries. *Circulation*. 2002;105:470-6.
27. Lamberts RR, Caldenhoven E, Lansink M, Witte G, Vaessen RJ, St Cyr JA, et al. Preservation of diastolic function in monocrotaline-induced right ventricular hypertrophy in rats. *Am J Physiol Heart Circ Physiol*. 2007;293:H1869-76.

28. Haddad F, Hunt SA, Rosenthal DN, Murphy DJ. Right ventricular function in cardiovascular disease, part I: anatomy, physiology, aging, and functional assessment of the right ventricle. *Circulation*. 2008;117:1436-48.
29. Burkhoff D, Mirsky I, Suga H. Assessment of systolic and diastolic ventricular properties via pressure-volume analysis: a guide for clinical, translational, and basic researchers. *Am J Physiol Heart Circ Physiol*. 2005;289:H501-12.
30. Faber MJ, Dalinghaus M, Lankhuizen IM, Steendijk P, Hop WC, Schoemaker RG, et al. Right and left ventricular function after chronic pulmonary artery banding in rats assessed with biventricular pressure-volume loops. *Am J Physiol Heart Circ Physiol*. 2006;291:H1580-6.
31. Dell'Italia LJ, Walsh RA. Application of a time varying elastance model to right ventricular performance in man. *Cardiovasc Res*. 1988;22:864-74.

Surg Today (2009) 39:133–136
DOI 10.1007/s00595-008-3803-x

SURGERY TODAY

Case Reports

Combined Autologous Cellular Cardiomyoplasty Using Skeletal Myoblasts and Bone Marrow Cells for Human Ischemic Cardiomyopathy with Left Ventricular Assist System Implantation: Report of a Case

SHIGERU MIYAGAWA[1], GORO MATSUMIYA[1], TOSHIHIRO FUNATSU[1], MASAO YOSHITATSU[1], NAOZUMI SEKIYA[1], SHINYA FUKUI[1], TAKAYA HOASHI[1], MASATSUGU HORI[2], HIDEKI YOSHIKAWA[3], YUZURU KANAKURA[4], JUN ISHIKAWA[4], KATSUYUKI AOZASA[5], NAOMASA KAWAGUCHI[6], NARIAKI MATSUURA[6], AKIRA MYOUI[7], AKIFUMI MATSUYAMA[7], SACHIKO EZOE[7], HIDEHIRO IIDA[8], HIKARU MATSUDA[9], and YOSHIKI SAWA[1]

[1]Division of Cardiovascular Surgery, Departments of Surgery, [2]Cardiovascular Medicine, [3]Orthopedics, [4]Hematology and Oncology, and [5]Pathology, [6]Department of Pathology, School of Allied Health Science, Faculty of Medicine, and [7]Medical Center for Translational Research, Osaka University Graduate School of Medicine, 2-2 Yamada-oka, Suita, Osaka 565-0871, Japan
[8]Department of Investigative Radiology, National Cardiovascular Center Research Institute, Suita, Osaka, Japan
[9]Department of Cardiovascular Surgery, Hyogo Medical College, Nishinomiya, Hyogo, Japan

Abstract
Myocardial regeneration therapy shows great promise as a treatment for heart failure. We recently introduced combined autologous cellular cardiomyoplasty with skeletal myoblasts and bone marrow cells as a treatment for human ischemic cardiomyopathy. We report the results of our first clinical trial of this technique, used to treat a patient with severe heart failure caused by ischemic cardiomyopathy who was being managed with a left ventricular assist system (LVAS). After combined cell transplantation, the patient showed signs of improved cardiac performance and angiogenesis, and reduced fibrosis.

Key words Cell transplantation · Heart failure · Left ventricular assist device

Introduction

Recent evidence shows that cellular cardiomyoplasty has potential fundamental regenerative capability, and it has already been introduced in clinical trials using skeletal myoblasts[1] or bone marrow mononuclear cells (BM-MNCs).[2] Myoblast transplantation offers a potential therapeutic treatment for end-stage heart disease with no risk of arrhythmia.[1] In one clinical trial, BM-MNCs were found to effectively treat acute myocardial infarction by enhancing angiogenesis.[2] Furthermore, an adequate supply of angiogenic and growth factors has an important adjuvant effect in cellular cardiomyoplasty, because reduced regional blood flow restricts myoblast survival and growth in ischemic cardiomyopathy.[3] We previously reported that myoblast grafting combined with BM-MNC transplantation in dogs enhanced both myogenesis and angiogenesis, leading to the restoration of myocardium damaged by ischemia.[4] Based on this evidence, we decided to use this therapy to assess the safety of combined cell therapy in patients with severe ischemic cardiomyopathy managed with left ventricular assist system (LVAS). To the best of our knowledge, this is the first report of a patient treated with both BM-MNCs and myoblasts after LVAS implantation.

Reprint requests to: Y. Sawa
Received: October 26, 2007 / Accepted: January 3, 2008

Case Report

A 53-year-old man with a history of two acute anterior myocardial infarctions suffered a third infarction of the left main trunk. The resulting cardiogenic shock was managed with percutaneous cardiopulmonary support (PCPS). He was weaned off PCPS in a few days but remained dependent on high-dose catecholamines. He had a large area of infarction in the left ventricular (LV) anterior and lateral wall and little viability was detected by Tl scintigraphy. Thus, combined cell therapy was approved by the Ethical Committee and Internal Review Board of Osaka University. After obtaining informed consent from the patient, a piece of skeletal muscle was excised from his medial vastus muscle and myoblasts were cultured according to published procedures.[1]

Table 1. Change in functional measures after cell transplantation (LVAS off test)

	Pre Tx	1 month after Tx	3 months after Tx
EF (%)	22	22.5	32
Dd/Ds (mm)	59/55	53/48	63/53
ABP (mmHg)	84/57 (69)	87/52 (65)	76/42 (51)
PAP (mmHg)	57/29 (41)	40/27 (34)	32/14 (28)
CI (l/min/kg)	2.09	1.76	1.7
SvO_2 (%)	55.5	60.6	60.7
CVP (mmHg)	13	11	7

LVAS, left ventricular assist system; Tx, cell transplantation; EF, ejection fraction; Dd/Ds, end-diastolic/end-systolic dimension; ABP, arterial blood pressure; PAP, pulmonary artery pressure; CI, cardiac index; SvO_2, venous oxygen saturation; CVP, central venous pressure

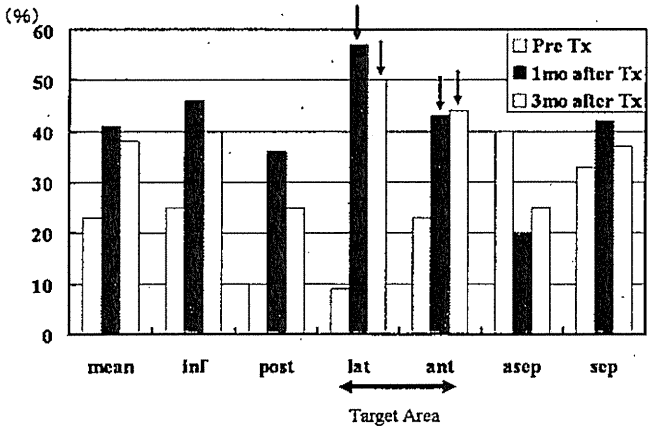

Fig. 1. The Color Kinesis index revealed restoration of regional diastolic function in the transplanted lesion in the anterior and lateral wall. *Arrows* indicate the improvement in regional diastolic function in the lesion post transplantation compared with the same lesion before transplantation. *Tx*, cell transplantation; *mo*, month; *inf*, inferior; *post*, posterior; *lat*, lateral; *ant*, anterior; *asep*, anteroseptal; *sep*, septal

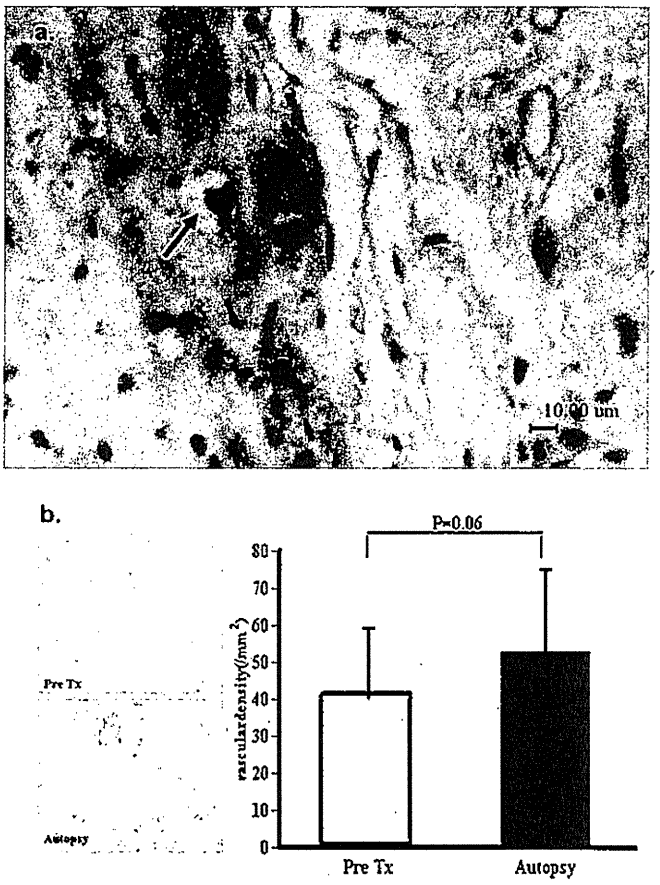

Fig. 2. **a** Detection of transplanted myoblasts. Fast-isoform myosin heavy chain-positive cells were detected in the transplantation site (*arrow*). **b** Induction of angiogenesis after cell transplantation. The number of vessels in the lesion was higher after cell transplantation than in the pre-cell-transplantation sample

Fluorescence-activated cell sorter (FACS) analysis with CD 56 antibody (BD, Rockville, MD, USA) revealed 46.6% purity of myoblasts. During the culture his heart failure worsened, so we performed left ventriculoplasty, as overwrapping, and mitral annuloplasty combined with extracorporeal pneumatic LVAS (Toyobo, Tokyo, Japan) implantation. About 3 months after this operation, we performed a left thoracotomy and, using a syringe, injected myoblasts (3×10^8 cells/3 ml) and BM-MNCs (1×10^8 cells/3 ml) separately into 30 points each, respectively, in the area of the transmural anterior and lateral myocardial infarction. We aspirated bone marrow from the ileum and sorted MNCs on a CS3000-Plus blood-cell separator (Baxter, Deerfield, IL, USA) according to published procedures.[5] The follow-up examinations showed a significant decrease in BNP, from 825 ± 565 pg/ml before to 275 ± 167 pg/ml after cell transplantation ($P < 0.05$), and an increase in the ejection fraction, from 22% before to 32% 3 months after cell transplantation in serial LVAS-off tests (Table 1). There was also an improvement in regional diastolic function, as assessed by the Color Kinesis index according to published procedures[6] (Fig. 1). No detrimental effects such as life-threatening arrhythmias were observed during follow-up. Unfortunately, the patient died of bacterial sepsis 466 days after surgery.

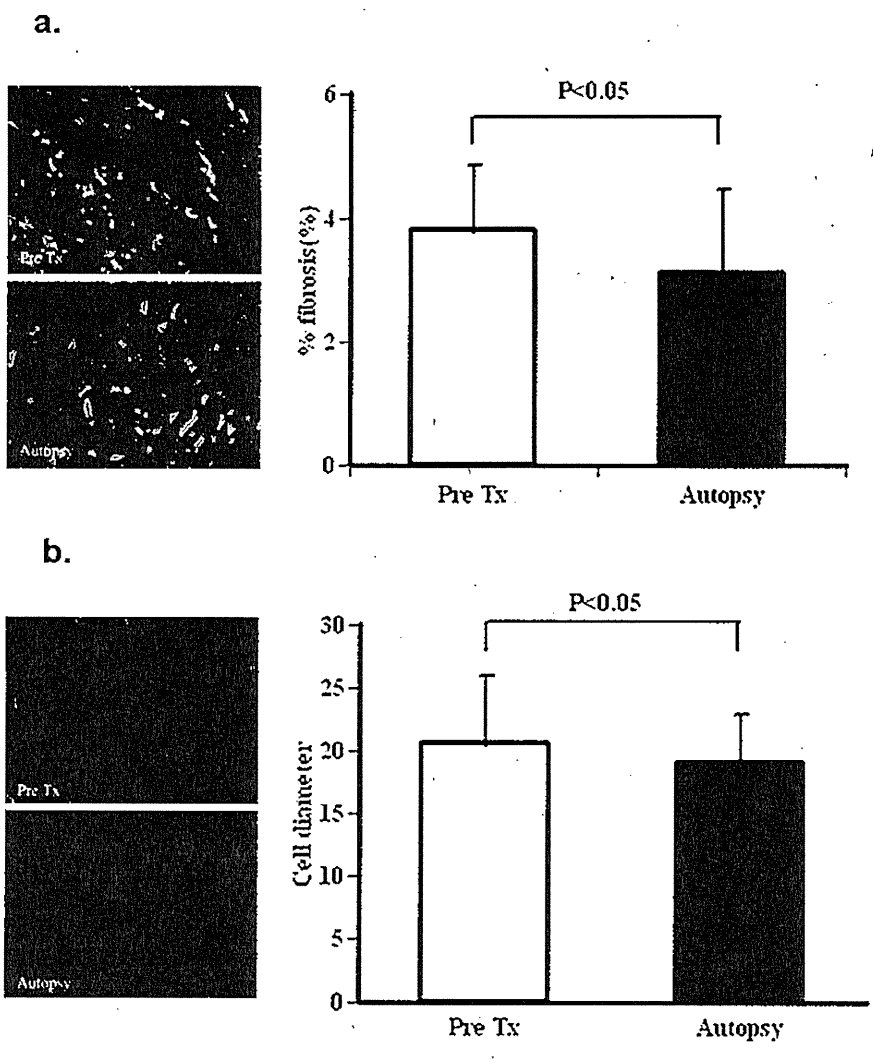

Fig. 3. a Reduction of percent fibrosis after cell transplantation. The percent fibrosis after cell transplantation was significantly lower than in the pre-cell-transplantation sample. **b** Shortening of the minor axis of host cardiomyocytes after cell transplantation. The hypertrophy of the host cardiomyocytes recovered remarkably compared with the pre-cell-transplantation sample

Immunostaining of fast-isoform myosin heavy chain (Sigma, St. Louis, MO, USA) of the autopsy sample revealed transplanted myoblasts in the site of transplantation (Fig. 2). Immunohistochemical staining of factor VIII-related antigen (DAKO EPOS Anti-Human Von Willebrand Factor/HRP; DAKO, Glostrup, Denmark) revealed that vascular density was higher (LVAS implantation vs autopsy = 40.53 ± 22.09/mm^2 vs 52.82 ± 18.72/mm^2; $P = 0.06$), the percent fibrosis (Masson's trichrome stain) was significantly lower (LVAS implantation vs autopsy = 3.78% ± 1.08% vs 3.11% ± 1.35%; $P < 0.05$) (Fig. 3) and the cell diameter was significantly shorter (LVAS implantation vs autopsy = 20.55 μm ± 5.37 μm vs 18.89 μm ± 3.98 μm; $P < 0.05$) than in samples obtained at the time of LVAS implantation.

Discussion

We decided to perform combined cell therapy instead of single cell therapy for this patient based on our finding that combined cell therapy has a more synergistic effect on severely damaged myocardium. To our knowledge, this is the first case in which both myoblasts and BM-MNCs were transplanted into human ischemic myocardium in a patient managed with LVAS, and recovery of cardiac function and histological changes were observed. However, we could not establish if the dramatic functional improvement was attributable to decreased LV distension by LVAS or to the cell transplantation because of the lack of an appropriate control. The BNP levels were significantly lower after cell transplantation than under LVAS before cell transplantation. For patients with ischemic cardiomyopathy, LVAS implantation does not achieve sufficient recovery of myocardial function.[7] Thus, we assume that the increased cardiac function was due to cell transplantation, although further clinical studies must be done to analyze the effects of cell transplantation. After LVAS implantation, decreased LV distension contributed to the reduced cell diameter and lower BNP, in accordance with previous reports. We detected other changes such

as improved regional diastolic function and vascular density in the targeted region in addition to the changes evoked by LVAS implantation. This indicates that cell transplantation had a positive effect on the distressed ischemic myocardium.

Enhanced expression of angiogenic factors by the transferred cells might induce angiogenesis and reduce fibrosis. We speculated that the transplanted cells, which have high elasticity, survived in the ischemic myocardium and may have contributed to regional diastolic improvement at the site of transplantation. Thus, combined therapy with myoblast and BM-MNCs transplantation could become part of the armamentarium of regenerative therapies for severely damaged ischemic myocardium.

References

1. Dib N, Michler RE, Pagani FD, Wright S, Kereiakes DJ, Lengerich R, et al. Safety and feasibility of autologous myoblast transplantation in patients with ischemic cardiomyopathy: four-year follow-up. Circulation 2005;112(12):1748–55.
2. Perin EC, Dohmann HF, Borojevic R, Silva SA, Sousa AL, Mesquita CT, et al. Transendocardial, autologous bone marrow cell transplantation for severe, chronic ischemic heart failure. Circulation 2003;107(18):2294–302.
3. Miyagawa S, Sawa Y, Taketani S, Kawaguchi N, Nakamura T, Matsuura N, et al. Myocardial regeneration therapy for heart failure: hepatocyte growth factor enhances the effect of cellular cardiomyoplasty. Circulation 2002;105(21):2556–61.
4. Memon IA, Sawa Y, Miyagawa S, Taketani S, Matsuda H. Combined autologous cellular cardiomyoplasty with skeletal myoblasts and bone marrow cells in canine hearts for ischemic cardiomyopathy. J Thorac Cardiovasc Surg 2005;130(3):646–53.
5. Tateishi-Yuyama E, Matsubara H, Murohara T, Ikeda U, Shintani S, Masaki H, et al. Therapeutic angiogenesis for patients with limb ischaemia by autologous transplantation of bone-marrow cells: a pilot study and a randomised controlled trial. Lancet 2002;10; 360(9331):427–35.
6. Ishii K, Miwa K, Makita T, Okuda N. Prolonged postischemic regional left ventricular delayed relaxation or diastolic asynchrony detected by color kinesis following coronary vasospasm. Am J Cardiol 2003;91(11):1366–69.
7. Mancini DM, Beniaminovitz A, Levin H, Catanese K, Flannery M, DiTullio M, et al. Low incidence of myocardial recovery after left ventricular assist device implantation in patients with chronic heart failure. Circulation 1998;98:2383–9.

J Artif Organs (2009) 12:187–193
DOI 10.1007/s10047-009-0465-4

ORIGINAL ARTICLE

Yukiko Imanishi, PhD · Shigeru Miyagawa, MD, PhD
Satoru Kitagawa-Sakakida, MD, PhD
Satoshi Taketani, MD, PhD · Naosumi Sekiya, MD
Yoshiki Sawa, MD, PhD

Impact of synovial membrane-derived stem cell transplantation in a rat model of myocardial infarction

Abstract To explore a new source of cell therapy for myocardial infarction (MI), we assessed the usefulness of mesenchymal stem cells derived from synovial membrane samples (SM MSCs). We developed a model of MI by ligation of the proximal left anterior descending coronary artery (LAD) in Lewis rats. Two weeks after ligation, 5×10^6 SM MSCs were injected into the MI scar area (T group, $n = 9$), while buffer was injected into the control group (C group, $n = 9$). Cardiac performances measured by echocardiography at 4 weeks after transplantation were significantly increased in the T group as compared with the C group. Masson's trichrome staining showed that SM MSC transplantation decreased collagen volume in the myocardium. Engrafted SM MSCs were found in the border zone of the infarct area. Immunohistological analysis showed that these cells were positive for the sarcomeric markers alpha-actinin and titin, and negative for desmin, troponin T, and connexin 43. SM MSC transplantation improved cardiac performance in a rat model of MI in the subacute phase, possibly through transdifferentiation of the engrafted cells into a myogenic lineage, which led to inhibition of myocardial fibrosis. Our results suggest that SM MSCs are a potential new regeneration therapy candidate for heart failure.

Key words Myocardial infarction · Synovial membrane · Mesenchymal stem cells · Cell transplantation

Introduction

Despite advances in medical and surgical procedures, congestive heart failure remains a leading cause of cardiovascular morbidity and mortality. Recently, autologous cell therapy methods using skeletal myoblasts or bone-marrow-derived cells for end-stage heart failure have been examined in clinical phase trials.[1–3] Although controversy remains regarding the exact mechanism of therapeutic gain, it is suggested that donor skeletal myoblasts differentiate into myogenic lineage, and suppress left ventricular (LV) dilation following myocardial infarction (MI).[4,5] However, it is also reported that transplanted skeletal myoblasts may be a trigger of arrhythmia.[6] On the other hand, the transplanted bone-marrow-derived cells release cytokines as vascular endothelial growth factor (VEGF), which induce angiogenesis in the infarct myocardium and improve cardiac performance indirectly via reconstitution of blood flow.[2,7,8] As for cell differentiation, bone-marrow-derived cells contain very few stem cells that are able to transdifferentiate into cardiomyocytes, but it is unlikely that such rare and spontaneous transdifferentiation can compensate for necrotic cardiomyocytes.[9] For regeneration therapy, it is important to search for more suitable cell sources that have properties similar to cardiomyocytes without arrhythmogenesis.

Mesenchymal stem cells derived from synovial membrane sample (SM MSC) are reported to have multilineage differentiation potential such as myocytes, adipocytes, chondrocytes, and osteocytes in vitro.[10] Furthermore, in vivo it is reported that SM MSC can attach to the hind limb as a functional satellite cell that is ready to differentiate into skeletal myocytes for muscle injury.[11] Those findings suggest that SM MSCs are more immature than skeletal satellite cells and their plasticity allows differentiation into a suitable lineage based on environmental cues. In this study, we assessed the therapeutic efficacy of SM MSC transplantation in a model of subacute phase myocardial infarction (MI), which showed moderate fibrosis, LV dilation, and remodeling. MI hearts in this stage have the potential to recover from heart failure.[12,13] We analyzed the transdifferentiation of cardiomyogenic lineage and compensation for lost contractility of the transplanted SM MSCs to evaluate their utility as a novel cell source for regeneration therapy.

Received: December 25, 2008 / Accepted: April 16, 2009

Y. Imanishi · S. Miyagawa · S. Kitagawa-Sakakida · S. Taketani · N. Sekiya · Y. Sawa (✉)
Division of Cardiovascular Surgery, Department of Surgery, Osaka University Graduate School of Medicine, E1 2-2 Yamada-oka, Suita, Osaka 565-0871, Japan
Tel. +81-66-879-3154; Fax +81-66-879-3163
e-mail: sawa@surg1.med.osaka-u.ac.jp

Materials and methods

Humane animal care was used in compliance with the *Principals of Laboratory Animal Care* formulated by the National Society for Medical Research, and the *Guide for the Care and Use of Laboratory Animals* prepared by the Institute of Laboratory Animal Resource and published by the National Institute of Health (NIH publication No.85–23, revised 1996).

SM MSC preparation and culture

Synovial membranes were obtained aseptically from the knee joints of Lewis rats (male, weighing 220–250 g). SM MSCs were isolated and expanded in monolayers on plastic dishes in growth medium (Dubecco's modified Eagle's medium, DMEM; Invitrogen, Carlsbad, CA, USA) containing 10% fetal bovine serum (FBS) and antibiotics (Gibco), as described previously.[10] After 3 to 5 passages, SM MSCs were washed with phosphate-buffered saline, harvested by incubation with 0.25% trypsin (Gibco) at 37°C for 5 min, washed with Hanks' balanced saline solution (HBSS; Sigma-Aldrich, St. Louis, CA, USA), and adjusted to 5×10^6 cells in 200 µl of HBSS for cell transplantation.

Myocardial infarction model

Isogenic male Lewis rats weighing 220–250 g (Kyudo, Hukuoka, Japan) were used as donors and recipients of SM MSCs to simulate autologous implantation. MI was produced by ligation of the proximal left anterior descending coronary artery (LAD), as described previously.[12] Two weeks after ligation, the rats were used as a model of heart failure due to MI, which is a subacute phase of MI, in which moderate fibrosis and diminishing inflammation is found.

SM MSC transplantation

SM MSCs were injected into the infarcted area 2 weeks after LAD ligation using a 30-G tuberculin syringe. The recipient rats were anesthetized and the thorax was opened at the fifth left intercostal space to expose the heart. We injected a total of 5×10^6 SM MSCs suspended in 200 µl of HBSS (therapeutic group: T group), or HBSS alone (sham-operated control group: C group), into the myocardium at five points using a 30-gauge needle ($n = 9$ each group). To detect donor cells, SM MSCs were labeled with fluorescent dyes using a PKH26 red fluorescent cell linker kit (Sigma) before transplantation.

Myocardial echocardiography

Echocardiographic studies were performed by an investigator blinded to treatment group allocation. The studies were performed before ligation, 2 weeks after ligation (before treatment), and 4 weeks after cell transplantation (after treatment). Two-dimensional, targeted M-mode tracings were obtained at the level of the papillary muscles with an echocardiographic system equipped with a 12-MHz transducer (SONOS 5500; Philips, Amsterdam, The Netherlands). Left ventricular (LV) dimensions were measured according to the American Society for Echocardiology leading-edge method from at least three consecutive cardiac cycles. The LV ejection fraction (LVEF) was calculated as $(LVDd^3 - LVDs^3)/LVDd^3 \times 100$, where LVDd is the LV endodiastolic dimension and LVDs is the LV endosystolic dimension. The LV fractional area change (LVFAC) was calculated as (LVEDA–LVESA)/LVEDA × 100, where LVEDA is the LV endodiastolic area and LVESA is the LV endosystolic area.

Histological analysis

All rats were humanely killed 4 weeks after cell transplantation. LV samples were cut transversely into four equal slice samples. To detect fibrosis, the LV myocardium was fixed in 10% formalin and embedded in paraffin and stained with Masson's trichrome. Ten randomly selected fields per section were analyzed using MetaMorph software (Nippon Roper, Tokyo, Japan). The collagen volume fraction was calculated as the sum of all areas containing connective tissue divided by the total area of the image. For immunohistochemical analysis, the specimens were embedded in OCT compound, snap-frozen in liquid N_2, cut into 5-µm sections, and fixed with 4% paraformaldehyde (Wako, Osaka, Japan). Immunofluorescence staining was performed with monoclonal mouse anti-alpha-actinin sarcomeric (Sigma-Aldrich), anti-titin (Sigma-Aldrich), anti-desmin (DakoCytomation, Glostrup, Denmark), anti-troponin T (Neo Markers Fremont, CA, USA), and anti-connexin 43 (Millipore, Bedford, MA, USA). Alexa488-conjugated IgG antibody (Invitrogen) was used as a secondary antibody, while 4′-6-diamidino-2-phenylindole (DAPI; Dojindo, Kumamoto, Japan) was used for counter staining.

Data analysis

Data are expressed as the mean ± standard deviation. To assess the significance of the differences between individual groups, statistical comparison was performed using an unpaired *t*-test. A value of $P < 0.05$ was considered to be statistically significant.

Results

Cardiac performance in SM MSC transplanted MI rats

An echocardiographic study confirmed that LAD ligation induced LV dysfunction, as indicated by LV dilation and lower contractility (before MI vs before treatment, Fig. 1 A–F). At the point of 2 weeks after ligation (pretreatment) and 4 weeks after transplantation (post-treatment), echocardiography was performed. Two weeks after ligation, LV

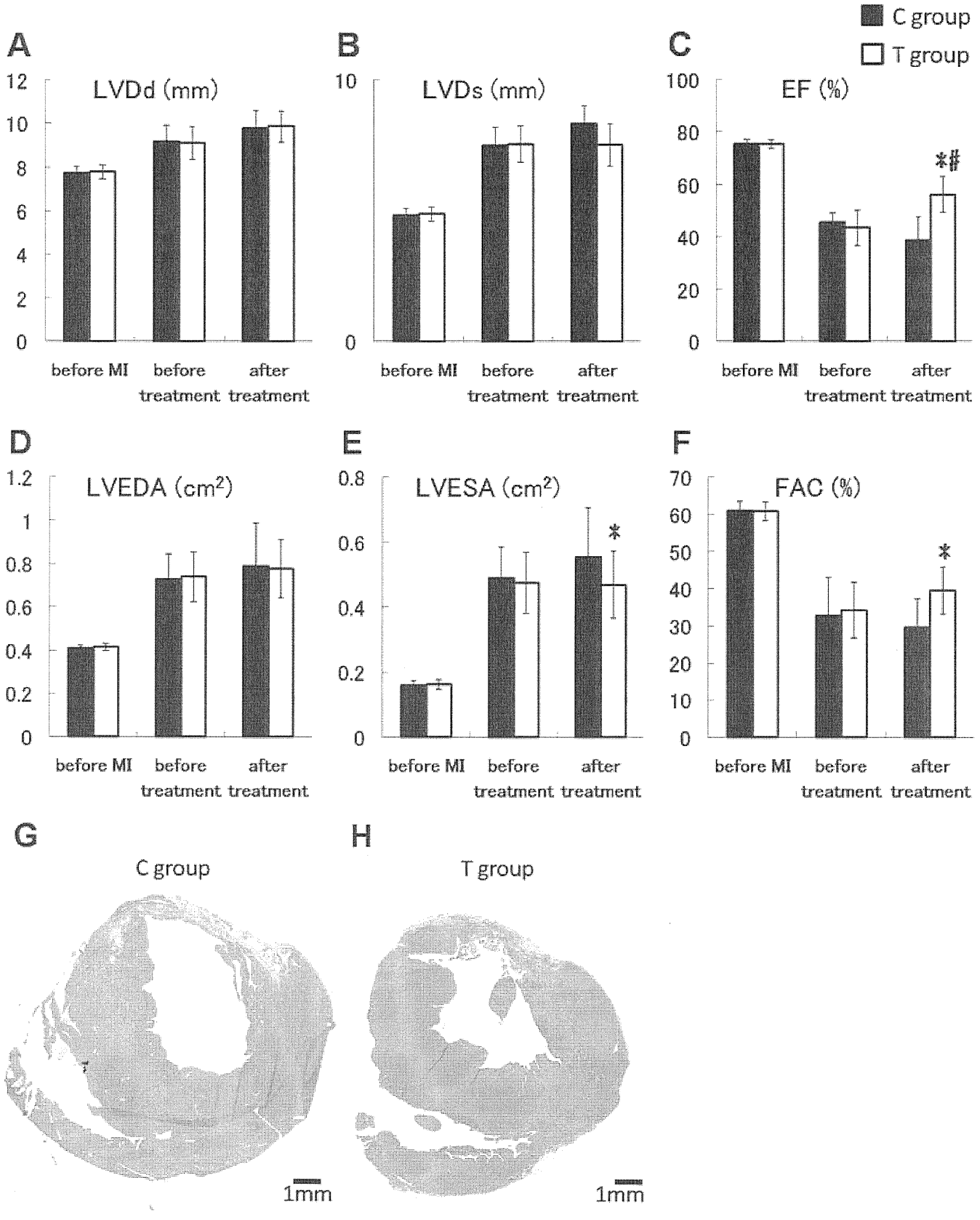

Fig. 1A–H. Cardiac performance of mesenchymal stem cells derived from synovial membrane samples (SM MSC) transplanted in myocardial infarction (*MI*) rats. **A** Left ventricular (LV) endodiastolic dimension (*LVDd*), **B** LV endosystolic dimension (*LVDs*), **C** LV ejection fraction (*LVEF*), **D** LV endodiastolic area (*LVEDA*), **E** LV endosystolic area (*LVESA*), and **F** LV fractional area change (*LVFAC*) were measured by echocardiography and calculated pretransplantation and 28 days post-transplantation. In T group, LVEF and LVFAC were significantly higher than C group after SM MSC transplantation. *Asterisk*, $P < 0.05$ vs C group; *hash*, $P < 0.05$ vs pretreatment. Image of typical whole hearts of C group (**G**) and T group (**H**). *Bars* 1 mm

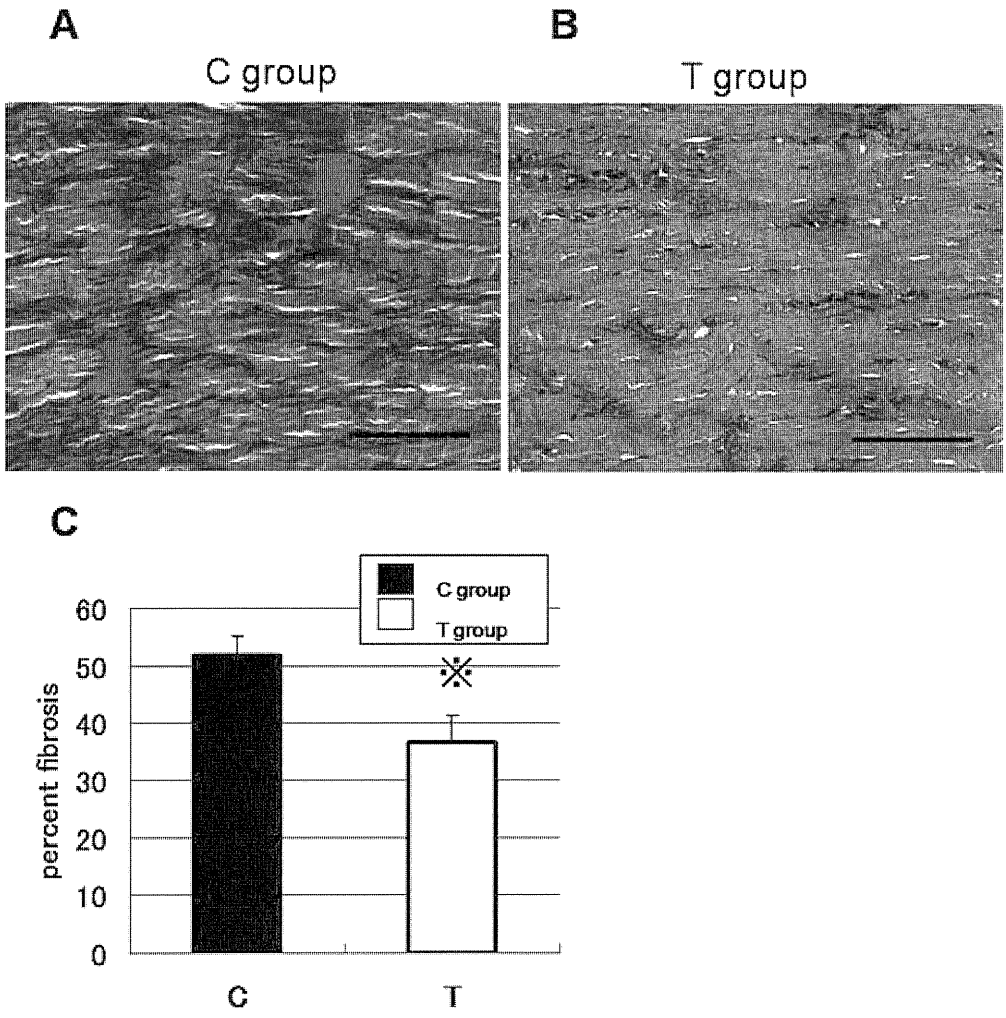

Fig. 2A–C. Effect of SM MSC transplantation on myocardial fibrosis. Typical histology of Masson's trichrome staining at border zone of C group (**A**) and T group (**B**). *Bars* 100 μm. **C** Quantification of collagen deposition at the border zone. The level of collagen deposition was lower in the T group than in the C group. *Asterisk*, $P < 0.05$ vs C group

dysfunction following MI was observed and there was no significant difference between both groups. Four weeks after treatment, in the C group, LV dysfunction seemed to be exacerbated as indicated by decreases in LVEF and LVFAC. In contrast, in the T group, exacerbation was attenuated. LVEF was significantly improved over pretreatment. Furthermore, LVEF and LVFAC of the T group were significantly higher than for the C group (Fig. 1A, B). This result was supported by macrohistological findings for the short axis images of the T group (Fig. 1D), which were showed small chambers and thick anterior walls of the LV when compared with the C group (Fig. 1D).

Myocardial fibrosis by SM MSC transplantation

Masson's trichrome staining demonstrated modest myocardial fibrosis at the border zone in the C group (Fig. 2A). In the T group, SM MSC transplantation attenuated fibrosis (Fig. 2B). Quantitative analysis also demonstrated that the collagen volume fraction in the T group was significantly lower than for the C group.

Survival and differentiation of engrafted SM MSCs in infarct heart

Four weeks after transplantation, the SM MSCs existed in the injected area of the T group. In particular, it was localized in the zone bordering the myocardium, but not in the myocardium. The morphology of the engrafted cells was small, round, and mononuclear. No vascular or capillary components were observed in the donor SM MSCs (Fig. 3A–C). Immunohistochemistry demonstrated that nearly all of the transplanted SM MSCs were positive for the myogenic markers alpha-actinin sarcomeric (Fig. 3D, E) and titin (Fig. 3F, G), while they were negative for desmin (Fig. 3H), troponin T (Fig. 3I), and connexin 43 (Fig. 3J).

Discussion

In this study, we demonstrated that cardiac performance was significantly improved by SM MSC transplantation (Fig. 1). SM MSCs transplantation (T group) induced a

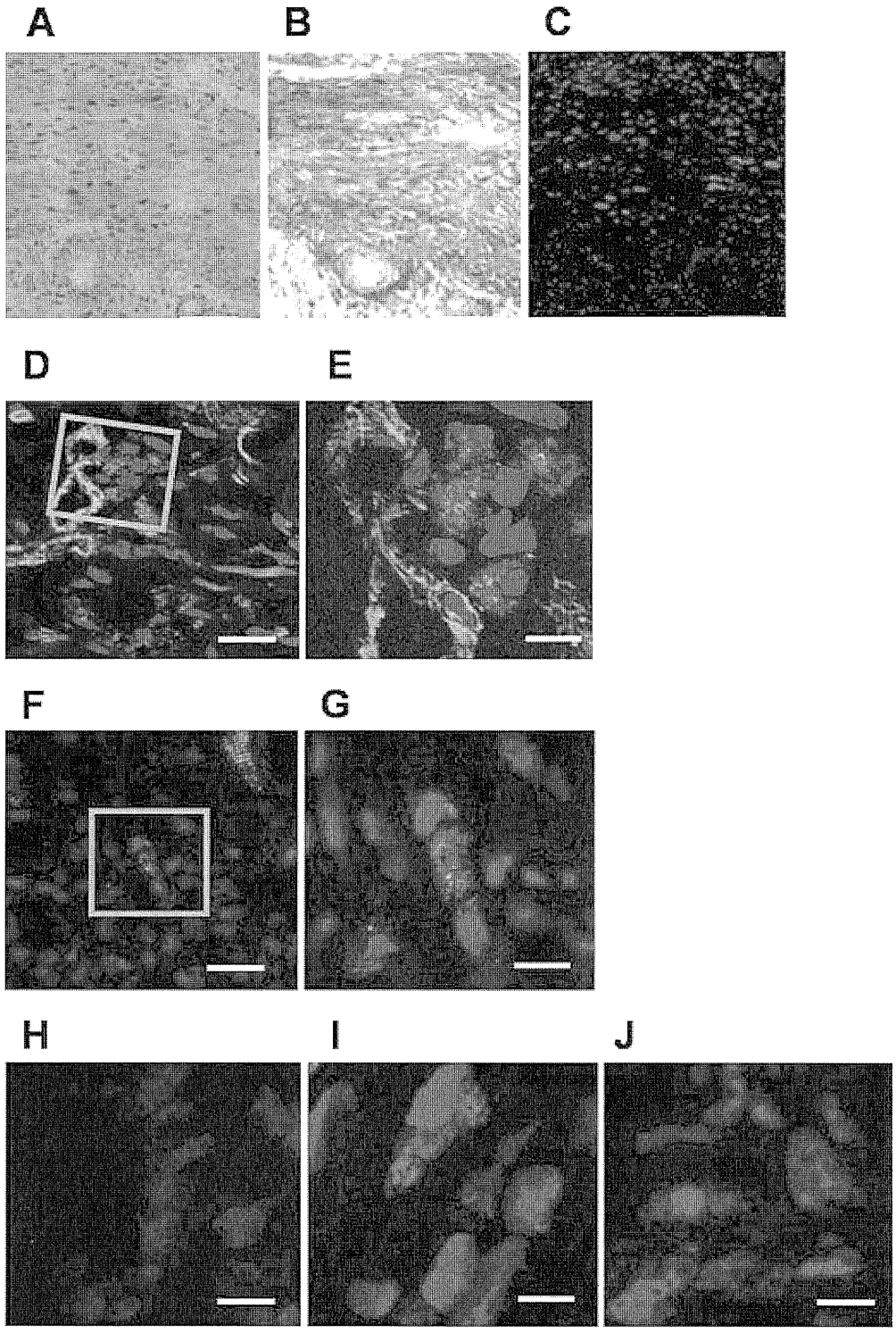

Fig. 3A–J. Survival and differentiation of engrafted SM MSCs in infarct heart. **A–C** Serial sections of infarct area of T group rat heart. **A** Hematoxylin-Eosin staining, **B** Masson's trichrome staining, **C** Sarcomeric alpha-actinin staining, *bars* 500 μm. **D** Sarcomeric alpha-actinin staining, *bar* 50 μm. **E** High-power magnification of square in **D**, *bar* 20 μm. **F** Titin staining, *bar* 50 μm. **G** High-power magnification of square in **F**, *bar* 20 μm. **H** desmin staining, **I** troponin T staining, **J** connexin 43 staining, *bars* 20 μm. *Red*, PKH26 labeled SM MSCs; *green*, conjugation with antibody; *blue*, nuclei

decrease of the LV fibrosis as compared with the sham-operated C group (Fig. 2). Furthermore, engrafted SM MSCs in infarct hearts of the T group expressed some sarcomeric proteins (Fig. 3). These findings suggest that SM MSC transplantation improves cardiac performance by partial transdifferentiation of the engrafted cells into a myogenic lineage in the area of infarction.

This is the first study to assess the therapeutic efficacy of SM MSCs following their transplantation into infarcted hearts. An increasing number of reports have shown that somatic stem cells can be isolated from various adult mesenchymal tissues, such as the synovium,[10] skeletal muscle,[14] and adipose tissue,[15] in addition to bone marrow.[16] SM MSCs are considered to be superior to other MSCs in mul-

tipotency and proliferation potential.[17] The synovium is an attractive source of MSCs, because it is easily regenerated after harvesting and readily available for clinical applications. It can be easily obtained arthroscopically with minimal invasiveness and without causing complications at the donor site, because the synovium has a high regenerative capacity.[18] A previous study demonstrated that an average of 21 000 cells per milligram of synovium collected were obtained after the nucleated cells were plated at optimal density and cultured for 14 days.[17] In a clinical trial, 1×10^7 to 1×10^8 cells were used for transplantation to MI patients.[19] A small sample of synovium harvested using a punch biopsy technique would be sufficient to obtain an adequate number of cells for future treatments.

MSC of bone marrow (BM MSC) is a popular cell source of regeneration therapy, which secretes angiogenic and antiapoptotic cytokines in infarct heart, but it merely transdifferentiates into cardiomyocytes.[20,21] On the other hand, most of the SM MSCs transplanted into the infarct myocardium expressed alpha-actinin (sarcomeric) and titin. Both paracrine factor and transdifferentiation of SM MSC might play a pivotal role in vivo. These events as cardiomyocyte apoptosis, reducing anterior wall thickness, increasing wall stress, and further cardiomyocyte death following LAD ligation might be prevented by cell transplantation. Although it is difficult to compare the fibrosis level of the same rat, it is likely that the exacerbation after MI was attenuated by SM MSC transplantation.

We found that the transplanted SM MSCs had partially differentiated into a myogenic lineage, but not into mature cardiomyocytes. This means cell fusion between engrafted SM MSC and native cardiomyocyte did not occur, but rather transdifferentiation of SM MSC into myogenic lineage. It is unclear whether improvement of cardiac performance was exclusively caused by transdifferentiation of the engrafted cells, but it unlikely that only immature differentiation of donor cells could contribute therapeutic gain. Some recent reports have indicated that cell transplantation indirectly contributes a therapeutic effect via a paracrine effect.[22–24] The native cells activated by cell transplantation may repair cardiomyocytes and vessels injured by infarction. In addition, growth factors secreted by transplanted cells also mediate myocardial protection, which results in functional improvement.[1–3] Fibroblasts lining the synovial membrane have been reported to be an abundant source of cytokines in rheumatoid arthritis patients.[25,26] SM MSC transplantation may also induce angiogenesis in infarct myocardium. Recently, new techniques of cell-based artificial organs have been reported.[5,27,28] For example, our group have reported that sheet-shaped myoblasts have a great therapeutic effect for heart failure.[5,28–30] This study shows that SM MSCs are one of the promising candidates as a cell source of the new cell-based artificial organ for repair of heart failure.

Further analysis of the mechanism will be helpful to investigate new cell sources and in basic research for development of new drugs for MI. In conclusion, we demonstrated that SM MSC transplantation has therapeutic potential in myocardial infarction. It is very significant in the progress of regeneration therapy to find such a new cell source of other somatic stem cells.

References

1. Psaltis PJ, Zannettino AC, Worthley SG, Gronthos S. Concise review: mesenchymal stromal cells: potential for cardiovascular repair. Stem Cells 2008;26:2201–2210
2. Kinnaird T, Stabile E, Burnett MS, Epstein SE. Bone-marrow-derived cells for enhancing collateral development: mechanisms, animal data, and initial clinical experiences. Circ Res 2004;95: 354–363
3. Wollert KC, Drexler H. Cell-based therapy for heart failure. Curr Opin Cardiol 2006;21:234–239
4. Tambara K, Sakakibara Y, Sakaguchi G, Lu F, Premaratne GU, Lin X, Nishimura K, Komeda M. Transplanted skeletal myoblasts can fully replace the infarcted myocardium when they survive in the host in large numbers. Circulation 2003;108: II259–263
5. Kondoh H, Sawa Y, Miyagawa S, Sakakida-Kitagawa S, Memon IA, Kawaguchi N, Matsuura N, Shimizu T, Okano T, Matsuda H. Longer preservation of cardiac performance by sheet-shaped myoblast implantation in dilated cardiomyopathic hamsters. Cardiovasc Res 2006;69:466–475
6. Menasche P, Hagege AA, Vilquin JT, Desnos M, Abergel E, Pouzet B, Bel A, Sarateanu S, Scorsin M, Schwartz K, Bruneval P, Benbunan M, Marolleau JP, Duboc D. Autologous skeletal myoblast transplantation for severe postinfarction left ventricular dysfunction. J Am Coll Cardiol 2003;41:1078–1083
7. Iba O, Matsubara H, Nozawa Y, Fujiyama S, Amano K, Mori Y, Kojima H, Iwasaka T. Angiogenesis by implantation of peripheral blood mononuclear cells and platelets into ischemic limbs. Circulation 2002;106:2019–2025
8. Uemura R, Xu M, Ahmad N, Ashraf M. Bone marrow stem cells prevent left ventricular remodeling of ischemic heart through paracrine signaling. Circ Res 2006;98:1414–1421
9. Ying QL, Nichols J, Evans EP, Smith AG. Changing potency by spontaneous fusion. Nature 2002;416:545–548
10. De Bari C, Dell'Accio F, Tylzanowski P, Luyten FP. Multipotent mesenchymal stem cells from adult human synovial membrane. Arthritis Rheum 2001;44:1928–1942
11. De Bari C, Dell'Accio F, Vandenabeele F, Vermeesch JR, Raymackers JM, Luyten FP. Skeletal muscle repair by adult human mesenchymal stem cells from synovial membrane. J Cell Biol 2003;160:909–918
12. Miyagawa S, Sawa Y, Taketani S, Kawaguchi N, Nakamura T, Matsuura N, Matsuda H. Myocardial regeneration therapy for heart failure: hepatocyte growth factor enhances the effect of cellular cardiomyoplasty. Circulation 2002;105:2556–2561
13. Fukui S, Kitagawa-Sakakida S, Kawamata S, Matsumiya G, Kawaguchi N, Matsuura N, Sawa Y. Therapeutic effect of midkine on cardiac remodeling in infarcted rat hearts. Ann Thorac Surg 2008;85:562–570
14. Cao B, Zheng B, Jankowski RJ, Kimura S, Ikezawa M, Deasy B, Cummins J, Epperly M, Qu-Petersen Z, Huard J. Muscle stem cells differentiate into haematopoietic lineages but retain myogenic potential. Nat Cell Biol 2003;5:640–646
15. Zuk PA, Zhu M, Ashjian P, De Ugarte DA, Huang JI, Mizuno H, Alfonso ZC, Fraser JK, Benhaim P, Hedrick MH. Human adipose tissue is a source of multipotent stem cells. Mol Biol Cell 2002; 13:4279–4295
16. Prockop DJ. Marrow stromal cells as stem cells for nonhematopoietic tissues. Science 1997;276:71–74
17. Sakaguchi Y, Sekiya I, Yagishita K, Muneta T. Comparison of human stem cells derived from various mesenchymal tissues: superiority of synovium as a cell source. Arthritis Rheum 2005;52: 2521–2529
18. Pei M, He F, Vunjak-Novakovic G. Synovium-derived stem cell-based chondrogenesis. Differentiation 2008;76:1044–1056
19. Segers VF, Lee RT. Stem-cell therapy for cardiac disease. Nature 2008;451:937–942

20. Nygren JM, Jovinge S, Breitbach M, Sawen P, Roll W, Hescheler J, Taneera J, Fleischmann BK, Jacobsen SE. Bone marrow-derived hematopoietic cells generate cardiomyocytes at a low frequency through cell fusion, but not transdifferentiation. Nat Med 2004; 10:494–501
21. Pittenger MF, Martin BJ. Mesenchymal stem cells and their potential as cardiac therapeutics. Circ Res 2004;95:9–20
22. Dawn B, Stein AB, Urbanek K, Rota M, Whang B, Rastaldo R, Torella D, Tang XL, Rezazadeh A, Kajstura J, Leri A, Hunt G, Varma J, Prabhu SD, Anversa P, Bolli R. Cardiac stem cells delivered intravascularly traverse the vessel barrier, regenerate infarcted myocardium, and improve cardiac function. Proc Natl Acad Sci USA 2005;102:3766–3771
23. Srivastava D, Ivey KN. Potential of stem-cell-based therapies for heart disease. Nature 2006;441:1097–1099
24. Reinecke H, Minami E, Zhu WZ, Laflamme MA. Cardiogenic differentiation and transdifferentiation of progenitor cells. Circ Res 2008;103:1058–1071
25. Karouzakis E, Neidhart M, Gay RE, Gay S. Molecular and cellular basis of rheumatoid joint destruction. Immunol Lett 2006;106: 8–13
26. Huber LC, Distler O, Tarner I, Gay RE, Gay S, Pap T. Synovial fibroblasts: key players in rheumatoid arthritis. Rheumatology 2006;45:669–675
27. Kutschka I, Chen IY, Kofidis T, Arai T, von Degenfeld G, Sheikh AY, Hendry SL, Pearl J, Hoyt G, Sista R, Yang PC, Blau HM, Gambhir SS, Robbins RC. Collagen matrices enhance survival of transplanted cardiomyoblasts and contribute to functional improvement of ischemic rat hearts. Circulation 2006;114: I167–173
28. Miyagawa S, Sawa Y, Sakakida S, Taketani S, Kondoh H, Memon IA, Imanishi Y, Shimizu T, Okano T, Matsuda H. Tissue cardiomyoplasty using bioengineered contractile cardiomyocyte sheets to repair damaged myocardium: their integration with recipient myocardium. Transplantation 2005;80:1586–1595
29. Memon IA, Sawa Y, Fukushima N, Matsumiya G, Miyagawa S, Taketani S, Sakakida SK, Kondoh H, Aleshin AN, Shimizu T, Okano T, Matsuda H. Repair of impaired myocardium by means of implantation of engineered autologous myoblast sheets. J Thorac Cardiovasc Surg 2005;130:1333–1341
30. Hata H, Matsumiya G, Miyagawa S, Kondoh H, Kawaguchi N, Matsuura N, Shimizu T, Okano T, Matsuda H, Sawa Y. Grafted skeletal myoblast sheets attenuate myocardial remodeling in pacing-induced canine heart failure model. J Thorac Cardiovasc Surg 2006;132:918–924

Long-Term Clinical Outcome of Atrial Isomerism after Univentricular Repair

Takaya Hoashi, M.D.,* Hajime Ichikawa, M.D., Ph.D.,* Norihide Fukushima, M.D., Ph.D.,* Takayoshi Ueno, M.D., Ph.D.,* Shigetoyo Kogaki, M.D., Ph.D.,† and Yoshiki Sawa, M.D., Ph.D.*

**Department of Cardiovascular Surgery; and †Department of Pediatrics, Osaka University Graduate School of Medicine, Osaka, Japan*

ABSTRACT ***Objectives:*** **We retrospectively reviewed the long-term outcome of atrial isomerism patients after Fontan completion.** ***Methods:*** **Since 1972, 58 patients underwent a palliative procedure prior to the Fontan-type operation. Twenty-eight out of 58 patients could not reach Fontan-type operation. Twenty-five patients underwent Fontan-type operation, and 12 of them expired less than five years after the Fontan completion. Eleven patients survived more than five years after the Fontan completion and were identified as long-term survivors. The mean follow-up period was 13 ± 5 years.** ***Results:*** **During follow-up period, four of the 11 patients expired. The actuarial survival rates at 10, 15, and 20 years after univentricular repair (UVR) were 100%, 71.4%, and 53.6%, respectively. The significant predictors of long-term survival by univariate analysis were the staged strategy ($p = 0.019$), total cavo-pulmonary connection with extracardiac conduit ($p = 0.019$), and the absence of postoperative common atrioventricular valve regurgitation ($p = 0.040$). Six out of the seven present survivors showed New York Heart Association class I activity. All present survivors' mean percutaneous oxygen saturation, mean pulmonary arterial pressure, pulmonary capillary wedge pressure, single ventricular end diastolic volume index, and single ventricular ejection fraction were 88.8 ± 6.8%, 11.0 ± 2.6 mmHg, 5.8 ± 2.0 mmHg, 104 ± 37 mL/m^2, and 52.0 ± 6.5%, respectively.** ***Conclusions:*** **There are still life-threatening problems 10 years after the UVR. However, the excellent performance status of the present long-term survivors suggests that these problems can all be overcome by the present strategies established for the Fontan-type operation.** doi: 10.1111/j.1540-8191.2008.00704.x *(J Card Surg 2009;24:19-23)*

The outcome of the Fontan-type operation (univentricular repair: UVR) for patients with atrial isomerism had not been satisfactory until recently.[1-4] However, due to technical modifications such as changing from an atrio-pulmonary connection to a total cavo-pulmonary connection with an extracardiac conduit (EC-TCPC), a staged Fontan strategy with a bidirectional cavo-pulmonary shunt (BDG), or a hemi-Fontan procedure, and successful surgical repair of concomitant malformations, such as common atrioventricular valve regurgitation (CAVVR) or total anomalous pulmonary venous connection (TAPVC) with or without pulmonary venous obstruction, the survival rate after UVR for atrial isomerism has improved.[5-7] The next goal is to improve the long-term quality of life in these patients. The purpose of this study is to review the long-term outcome and the clinical features of survivors with atrial isomerism more than five years after Fontan completion in a single institution.

Address for correspondence: Hazime Ichikawa, M.D., Ph.D., 2-2-E1, Yamadaoka, Suita, Osaka, 565-0871, Japan. Fax: +81-6-6879-3163; e-mail: ichikawa@surg1.med.osaka-u.ac.jp

MATERIALS AND METHODS

Patients

Surgical palliation for UVR was performed in 58 patients with atrial isomerism of the heart in Osaka University Medical School Hospital since 1972. Among these patients, 25 underwent UVR and 11 of them survived for more than five years. We defined these 11 patients as long-term survivors (Table 1). The mean follow-up period from the Fontan-type operation was 13 ± 5 years (range, six to 21 years).

Anatomy

The diagnosis of atrial isomerism was mainly derived from visual inspection of the morphology of the atrial appendage during palliative operations.[8] The ventricular morphology was right in 10 patients and left in one, and the type of atrial isomerism was right in six patients and left in five. The associated cardiovascular malformations were a common atrioventricular valve (CAVV) in nine patients, with moderate or severe regurgitation in three patients, absence of the inferior vena cava in four patients, coarctation of the aorta in one patient, a

TABLE 1
All Patients with Atrial Isomerism

Atrial Isomerism (n)	58
Mortality after palliation	28
Drop out	5
Fontan completion	25
Early death	5
Late death	7
Survived $\leq$ 5 years	2
Survived > 5 years	11

single coronary artery in one patient, and an extracardiac TAPVC in one patient (Table 2).

Surgical procedures

The mean age at Fontan-type operation was 9.3 ± 6.2 years. Palliative operations were performed an average of 1.7 ± 1.0 times (range, one to four times). The modifications of the Fontan-type operation included atrio-pulmonary connection (APC) in one patient, intra-atrial grafting (IAG) in two patients, total cavo-pulmonary shunt, termed the Kawashima operation,[9] in three patients, and EC-TCPC in five patients.

TABLE 2
Patient Characteristics

Diagnosis	Number
Atrial isomerism	
Right	6
Left	5
Ventricular morphology	
Right	10
Left	1
Great arteries	
DORV	6
d-TGA	5
Right aortic arch	1
Coarctation	1
Pulmonary artery	
Atresia	1
Stenosis	7
Great veins	
Bilateral SVC	2
PL SVC	3
IVC absence	4
Atrio-ventricular valve	
Common	9
With regurgitation	3
DIRV	2
Hypoplastic LSAVV	1
RSAVV atresia	1
Pulmonary vein	
Extracardiac TAPVC	1
Intracardiac TAPVC	1
With PVO	0
Coronary artery	
Single coronary artery	1

DORV = double outlet right ventricle; TGA = transposition of great arteries; SVC = superior vena cava; IVC = inferior vena cava; DIRV = double inlet right ventricle; TAPVC = total anomalous pulmonary venous connection; PVO = pulmonary venous obstruction.

TABLE 3
Surgical Procedures

Variable	Number
Palliative operation	
PA band	1
SP shunt	10
PA plasty	2
Coarctectomy	1
SVC-PA anastomosis (bi-directional Glenn shunt)	3
Kawashima as	
Staging palliation	1
Historically definitive operation	3
Fontan modification	
APC	1
IAR	2
EC-TCPC (Converted from another modifications)	5 (2)
Concomitant operation	
CAVV plasty	1
CAVV replacement	1

PA = pulmonary artery; SP = systemic-pulmonary; SVC = superior vena cava; APC = atrio-pulmonary connection; IAR = intra atrial routing; EC-TCPC = total cavo-pulmonary shunt with an extra cardiac conduit; CAVV = common atrioventricular valve.

Fenestration was placed in three patients. One of these fenestrations has not been closed. The concomitant operations were a CAVV replacement and a CAVV plasty (Table 3).

Data collection and statistical analysis

The pre- and postoperative data were collected from each patient's records of Osaka University Medical School Hospital. The postoperative hemodynamic data were collected from cardiac catheterization and echocardiogram reports. The late mortality was evaluated using the Kaplan-Meier method and was compared with age-matched nonisomerism patients who survived more than five years after UVR (n = 45) using a log-rank test. The values are expressed as the mean ± standard deviation and as ranges. The data were analyzed using Stat-View statistical software (SAS Institute Inc., Cary, NC, USA). A univariate risk analysis was performed with Student's *t*-test. A p-value less than 0.05 was set as the level of statistical significance.

RESULTS

Late mortality after the Fontan-type operation

Four out of 11 patients expired during the follow-up period. The actuarial survival at 10, 15, and 20 years after UVR were 100%, 71.4%, and 53.6%, respectively. Comparisons with the nonisomerism patients after the Fontan-type operation indicated that the survival rate of atrial isomerism patients tends to decline 10 years after the Fontan operation, although not to a statistically significant degree (log-rank: p = 0.210) (Fig. 1).

Predictors of long-term survival

An univariate analysis showed that: (1) a staged strategy with bidirectional cavo-pulmonary shunt or total

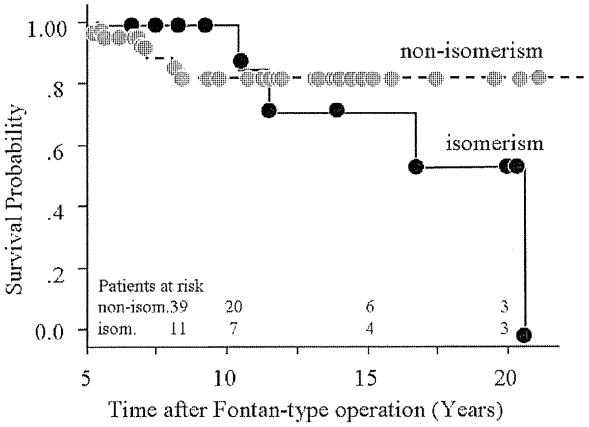

Figure 1. *Kaplan-Meier estimated actuarial survival of atrial isomerism and nonisomerism in patients who survived for more than five years after undergoing Fontan completion.*

cavo-pulmonary shunt, (2) EC-TCPC, and (3) absence of postoperative CAVVR were the significant predictive indices of survival. The type of atrial isomerism and the ventricular morphology showed no statistical significance (Table 4).

Clinical features of the long-term mortalities of four patients

All of the long-term mortalities were caused by cardiac-related problems. The survival durations of these four patients after the Fontan-type operation were 10.5, 11.5, 16.6, and 21.2 years. The ages of the patients at expiration were 13.6, 20.8, 27.3, and 44.6 years. The type of atrial isomerism was right in two patients and left in two patients. All patients had morphological right ventricles (Table 5).

TABLE 4
Predictors of Long-Term Survival

Factor	Survived (n = 7)	Expired (n = 4)	P Value
Staged strategy	5/7	0/4	0.019
EC-TCPC	5/7	0/4	0.019
Absence of post-operative CAVVR	7/7	2/4	0.040
Number of palliative operations	2.1 ± 1.1	1.0 ± 1.0	0.066
Age at initial operation	1.1 ± 2.8	4.3 ± 11.6	0.068
Pulmonary atresia	4/7	4/4	0.068
Post-operative arrhythmia	1/7	2/4	0.241
Post-operative cyanosis	1/7	2/4	0.241
Age at Fontan-type operation	7.7 ± 19.9	11.8 ± 78.3	0.332
IVC absence	2/7	2/4	0.527
Post-operative PAVMs	1/7	1/4	0.670
Right atrial isomerism	4/7	2/4	0.840
Single right ventricle	6/7	4/4	0.840

EC-TCPC = total cavo-pulmonary shunt; CAVVR = common atrioventricular valve regurgitation; IVC = inferior vena cava; PAVM = pulmonary arterio-venous malformation.

TABLE 5
Cause of Long-Term Mortality (n = 4)

No.	Isomerism (years)	Interval (years)	Expired Age	Postoperative Complications
1	Right	10.5	13.6	Ventricular failure CAVVR
2	Right	11.5	20.8	Ventricular failure, AT
3	Left	16.6	27.3	Severe cyanosis, AT
4	Left	21.2	44.6	Severe cyanosis, Ventricular failure CAVVR, AF

CAVVR = common atrioventricular valve regurgitation; AT = atrial tachycardia; AF = atrial fibrillation.

The first patient had a relatively large rudimentary left ventricular chamber, in which contractility deteriorated soon after APC without any sign of myocardial ischemia. CAVVR and dyssynchronized movement of the two ventricular chambers gradually progressed and resulted in the deterioration of right main ventricular contraction. Although a CAVV replacement and an implantation of a biventricular pacemaker were performed 13 years after the Fontan completion, the patient could not tolerate the procedure. An autopsy showed extensive fibrous change in the ventricular myocardium.

The second patient had no cyanosis or CAVVR after APC. Her ventricular ejection fraction (SVEF) progressively decreased from 59% at the operation to 20% six years after the operation. At the same time, she also suffered from atrial tachycardia (AT) attacks. She suddenly died at home 12 years after APC. The cause of ventricular failure remained unknown because an autopsy was not allowed.

The third patient suffered from severe cyanosis five years after a definitive Kawashima operation. Although coil embolizations were repeatedly performed for more than 20 pulmonary arteriovenous malformations (PAVMs), his cyanosis did not improve and promoted collateral vascularization, resulted in the occurrence of AT and failing ventricular performance. Severe cyanosis was the cause of this patient's mortality.

The fourth patient underwent CAVV replacement and Kawashima operation as a definitive UVR. The postoperative course was uneventful and she was able to successfully give birth. Thirteen years later, the prosthetic valve tissue degenerated and was replaced. Her cyanosis and ventricular failure gradually progressed. Finally this patient expired eight years after a repeat CAVV replacement, at the time she was undergoing an operation for infectious peritonitis.

Clinical features of present long-term survivors

Seven patients are now being followed-up. The mean follow-up period of the present survivors after the Fontan completion is 13.3 ± 5.9 years (range, 7.0 to 20.4 years) and the average age is 20.1 ± 9.2 years (range, 12.3 to 33.2 years of age). The clinical features of those seven patients were almost excellent (Table 6). Six patients showed New York Heart Association Class I activity. The mean percutaneous oxygen